A reconfigurable electrical circuit auto-processing method for direct electromagnetic inversion*

Jun LU[1][0000−0003−3009−6683]

Institute of Physics, Chinese Academy of Sciences / Beijing National Laboratory for Condensed Matter Physics, China lujun@iphy.ac.cn
http://www.iop.cas.cn/rcjy/yjdwfgj/?id=1784

Abstract. Extracting information as much and precise as possible from nondestructive measurements remains a challenge, especially when advanced test applications are emerging in electromagnetic encephalography and high throughput physical property characterization of materials genome chips. To solve the inversion problem, various soft algorithms have been developed such as finite element method, machine learning and artificial neural network, whose performance is limited by indirectly processing of intermediate layers in digital computers. This paper proposes a novel direct method of analog network entity with reconfigurable electrical circuit auto-processing(RECAP), which mainly consists of voltage controlled elements, measurement unit, and automatic feedback unit. During each inversion process, after the test results are input, the circuit network performs initialization, choosing topology, automatically tuning the property for each network element, and finally approaching a convergent solution to user request after some cycles of self-adjustment. Principles and advantages are introduced with several instances, showing high accuracy and stable convergence ability, as well as helping judge whether the topology is suitable for optimization. This method can not only inverse purely loss components, but also inverse circuits containing reactive components. Based on the verification from cases, it is also found that the inversion efficiency of RECAP is linearly dependent on the number of elements N, which is better than the usual mature inversion algorithms. Therefore, it is then concluded as a promising tool for high performance inversion.

Keywords: nondestructive testing · topological electrical circuit · electromagnetic inversion.

1 Introduction

The inversion problem was described by Langer as determination of equation coefficients followed by finding solution of the problem in 1930s[15]. Calderon

* This work is under supports from National Natural Science Foundation of China (No. 51327806), Fujian Institute of Innovation and Youth Innovation Promotion Association of Chinese Academy of Sciences (No.2018009).

clarified it as inverse boundary value problem [4]. Later, thanks to the introduction of regularization, complex practical inversion problems can also be simplified and solved [10]. Global uniqueness of inversion results is also possible if boundary has Lipshitz continuity for a 2D problem[19], 3D object[3] or system with higher dimension[28]. Inverse processing has been widely used in various engineering problems, especially electromagnetic related inversion, such as process coltrol[9], nondestructive detection or exploration[14][5][21][26], atomic resolution structural investigation[8][5][7], and biomedical characterization[31][22][12]. Many kinds of methods has been developed to solve electromagnetic inversion problems, including direct inversion[27] or asymptotic treatment[1], principle component analysis[29], statistical simulation[6], approximate finite elements analysis[11], and machine learning[17] even deep learning[16] in recent years. It is true that these inversion methods are pure digital algorithms where preprocessing and post-processing of data is necessary in computer. Moreover, calculation complexity of these inversion methods is polynomial dependent on number of basic blocks. Benner and Mach have proposed hierarchical process to reduce the time and storage cost, where the inverse complexity has been optimized to O(N*logN)[2]. In the case of large number of basic blocks, it is desirable to further reduce the processing complexity, since computation resources are limited. This paper is going to describe a new method for electromagnetic inversion, which can reduce the complexity further and hence possess high efficiency. The new method is based on reconfiguable electric circuits with precision measurement and automatic feedback. The concept of this reconfigurable electrical circuit auto-processing (RECAP) inversion process is merging test devices and the circuit under test, so as to directly inverse the original problem by self-adjusting each component in the network. Equivalent electrical circuits are usually used in simulation[13] and fitting software[24][32], or even for decryption[30]. Murai and Kagawa demonstrated 2D electric circuit network for a finite element solver[18], and Selleiri developed algorithms for topological optimization of circuit networks[25]. However, as far as the current author can concern, reconfigurable electrical circuits for automatical inversion have not been reported. Since quantum algorithms are crucial for the next generation computation and still under developing[20], the current paper is expected to provide a possible way for realizing the electromagnetic inversion of quantum optimization[23].

2 Principle Design

It has been an interesting but challenging problem to inverse all components of a electrical network without breaking any connection. The difficulty is not only from limited information on network topology, also from inevitable intercoupling, since single component can influence all impedance measurements and every two-node impedance result comes from the whole circuit network. Correspondingly, the proposed method compose of two levels of nested loops including main part level in the internal loop and topology selection level in the outer loop. The main inversion circuit contains measurement comparing part and

auto feedback adjustment part, where reconfigurable electrical network is composed of voltage tunable electronic components. As shown in Fig. 1, the outer loop performs topology selection, and the inner loop performs self-adjustment of component parameters for the set topology. In each set of topological structures, the parameters of the components can be adjusted by voltage, and the in-situ electrical properties at both ends of these variable electronic components are measured one by one. The measurement result is simultaneously compared with the measurement result of the inverse object circuit. The feedback voltage of the comparison result then controls the variable element to automatically adjust, and finally makes the in-situ measured electrical properties at both ends of the variable element is equal to that of the corresponding two end points of the inversion object circuit. The inversion operation of other components is subsequentially performed by the same procedures. When the comparison and feedback of all components in the set topology are finished, a round of RECAP inversion iteration is carried out. After that, it is judged whether to perform a new round of RECAP inversion iteration according to the relative error between the in-position measurement result and the inverse object, and the cycle repeats until the inversion result meets the stop error or reaches the maximum allowable number of iterations. When making optimization among multiple topological structures, it is necessary to compare the final relative error of the inversion iteration results of each structure, and select the topological structure with the lowest relative error. Finally, when the topological structure and all circuit components show acceptable consistent with the inversion object based on measurement of circuit properties, the whole inversion operation is completed.

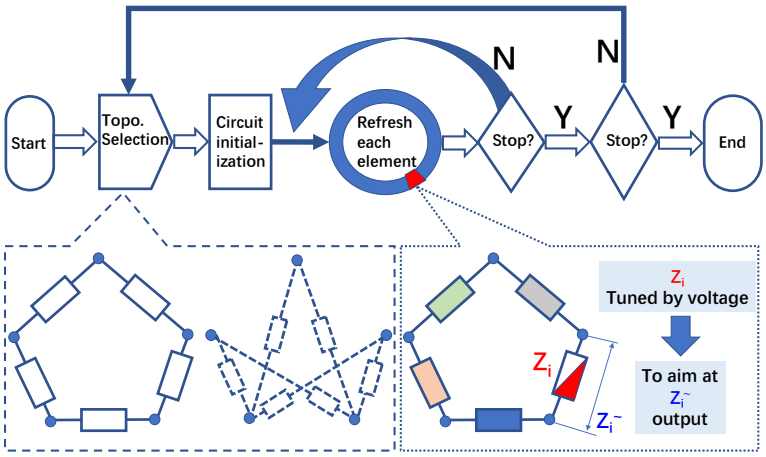

Fig. 1. Principle diagram of reconfigurable electrical circuit network for direct electromagnetic inversion.

3 Method Demonstration

In order to make the RECAP inversion method easier to be understood and applied, this section demonstrates the RECAP in a simple resistor network as an example for analysis. As shown in Fig. 2, a six-node, seven-element circuit network, each element is set with a resistance value Ri, and the resistance Ri' is directly measured in situ. The simulation results are shown in the table below the figure, where the first two data lines indicate that the difference between Ri and Ri' is very large. However, through the RECAP method, the set resistance value Ri of each element itself can be recovered after 3 iterations of inversion, and the average relative error $\sum_{i=1}^{N}[(Ri'-Ri)/Ri]/N$ is less than 1 %, where N is the total number of elements and i is each natural number between 1 and N (N=7 in the current demonstration). More cycles of inversion could be performed later, so as to obtain a lower relative error. The RECAP starts with initialization via selecting a measuring component. Under the constraint that all components are set to the same resistance, that is, the control terminals of all voltage variable resistors are connected to the same control terminal, and the voltage is adjusted to change the resistance of all components so that the apparent resistance of the two nodes of the measuring element is equal to the resistance of the corresponding nodes of the inversion object. Here, as the starting point, the resistance measured between nodes I and VI is 0.9 Ohm. By simulation tools such as LTSPICE one can find that when all resistances in the network are adjusted to 1.227 Ohms, the resistance measurement between nodes I and VI is 0.9 Ohms. Then RECAP continue moving the measurement probes of the resistance meter to the next element. After such initialization, the control ends of reconfigurable circuit components for all subsequent iterations are separated independently, that is, the RECAP component parameters are controlled and adjusted one by one. For example, the second comparison feedback element is connected to the nodes I and II, where the measured result of resistance between the nodes I and II of the inversion object circuit is 1.6 Ohms. To address the target resistance, the RECAP component between the nodes I and II is varied while all other resistances remain unchanged at 1.227 Ohms. Circuit simulation results show that the current iteration of the element is finished when the resistance increases to about 3 Ohms. Then the measurement probes is moved to nodes V and VI. As in the RECAP inversion procedures for the previous component connected between nodes I and II, the inversion result of the current iteration of the element is 4.75 Ohms. Sequentially, after performing such parameter reconstruction operation for all components of the target inversion circuit, the first round of inversion iteration is completed. At this time, it is judged whether the average relative error between the nodes of RECAP circuit and the corresponding nodes of the inversion object is acceptable. When the average relative error is larger than the set limit, such as 1% , the next round of inversion iteration is then proceeded. It can be seen from the inversion result data of this example that after the third round of inversion iteration, the average relative error of the inversion object has dropped below 1%. If more precision convergence is required, more inversion iterations will help to improve the inversion results.

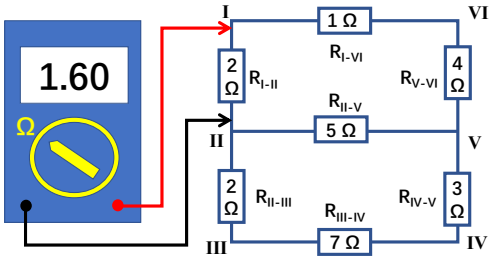

Unit: Ω	R_{I-VI}	R_{I-II}	R_{V-VI}	R_{II-V}	R_{II-III}	R_{IV-V}	R_{III-IV}
Set value	1	2	4	5	2	3	7
MeasRaw	**0.9**	**1.6**	**2.48**	**2.35**	**1.73**	**2.4**	**3.7**
InvRes-Cycle1	**1.227**	3.04225	4.75	23.23	2.144	3.17	5.39
InvRes-Cycle2	0.957	1.824	3.286	5.978	2.034	3.12	6.768
InvRes-Cycle3	0.99888	1.984	3.852	5.12	2	3.02	6.92
InvRes-Cycle4	0.995	1.975	3.99	5.05	1.999	3.01	6.933
InvRes-Cycle5	**0.994**	**1.969**	**4**	**5.04**	**1.999**	**3**	**6.934**

Fig. 2. A typical circuit for inverse demonstration, where each resistor component is in situ measured, and the entire measurement result is input to the reconfigurable circuit network. Under the RECAP inverse strategy, after 3 runs of auto adjustment, the inverse circuit inverses the set parameters within 1% uncertainty, and more iteration cycles afterwards can further improve the precision.

4 Evaluation And Discussion

4.1 Topological Determination

The determination of the topological structure is an interesting problem in electromagnetic inversion. It is found through the simulation results of cross-topology inversion that the RECAP method can not only select the best one from multiple topological structures based on the average relative error information, and it can also automatically detect whether the selected topology is correct, through the parameter evolution in the iterative process of topological structures with higher symmetry. This paper uses a four-node circuit network example to analyze, where the three topological networks a, b, and c of the four-node circuit shown in Fig. 3 have 4 components, 5 components, and 6 components, respectively. In order to better analyze the topological structures, each component parameter is set to equal resistance (here all resistances are 1 Ohm). The resistance between all two combination of the four nodes of the three topological structures has been listed in the table at the bottom of Fig. 3. As a result, it can be seen that the symmetry of the three topological structures with the same component parameters gradually increases from a to b to c.

When we use three different topological structures for the pairwise combination between RECAP and the three target circuits to be inversed, we obtain a

3x3 matrix, as shown in Fig. 4. Except for the diagonal combination of the topological cross matrix, where the inversion result is completely consistent with the set circuit, it is found that if a topology with a lower symmetry is used to inverse a target circuit with a higher symmetry, systemic errors will obviously occur. The error cannot be automatically judged without adding measurement information. Conversely, if a topology with higher symmetry is used to inverse a circuit with lower symmetry, the results of the inversed components are all correct, and the "excess" components will exhibit exponential divergence as the number of iterations increases. It can be seen that when a topology with a higher symmetry is used to inverse a circuit with a lower symmetry, RECAP can automatically determine that it uses an over-high symmetry. Obviously, for the topology inversion of RECAP, the recommended way is to start with high symmetry and reduce the symmetry gradually through clue from divergent components, so that the inversion results just do not appear divergent components.

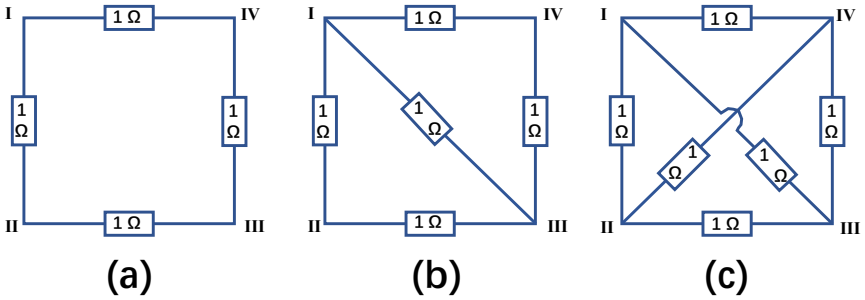

2T R	$R_{I\text{-}II}$	$R_{II\text{-}III}$	$R_{III\text{-}IV}$	$R_{IV\text{-}I}$	$R_{I\text{-}III}$	$R_{II\text{-}IV}$
(a)	0.75	0.75	0.75	0.75	1	1
(b)	0.625	0.625	0.625	0.625	0.5	1
(c)	0.5	0.5	0.5	0.5	0.5	0.5

Fig. 3. Four-node electrical circuit network with three topologies (a) a close loop with four resistors, (b) co-edge double triangles with five resistors, (c) a tetrahedron with six resistors, and the bottom table shows the raw resistance between nodes for three configurations.

4.2 Convergence Performance

When the topological structure is fixed, the convergence behavior during the electromagnetic inversion iteration process is a very interesting topic. It not only shows the evolution of the inversion accuracy, but also reflects whether the initialization process is reasonable. Through different set resistance parameters of the same topology, especially the change of the ratio of the maximum resistance to the minimum resistance, the simulation results are studied. As shown

in Fig. 5, ratios of the maximum to minimum resistance values of the inversion object are set 1, 10, and 1000 in Fig. 5 a, b, and c, respectively. For the resistor network with the same resistance, after the initialization operation of RECAP, the inversion result can be obtained from the beginning, and as the maximum to minimum resistance ratio increases, that is, the asymmetry of the inversion component parameters increases, and the circuit inversion iteration becomes slower. By changing the position of the initialization, the RECAP result also found that for the inversion object with low parameter symmetry, if the initial resistance is exactly selected at element where the smallest resistance locates, the result may not be converged. Nevertheless, when the initial position is selected at the highest resistance, as shown in Fig. 5 d and e, it is rather useful to obtain a stable iteration result. It is easier to perform RECAP initialization at a larger resistance to obtain a stable convergence result, mainly because the two-node resistance in the low resistance network has an upper limit of measured resistance, and it is impossible to obtain a higher resistance by adjusting the resistance of the component connected to these two nodes.

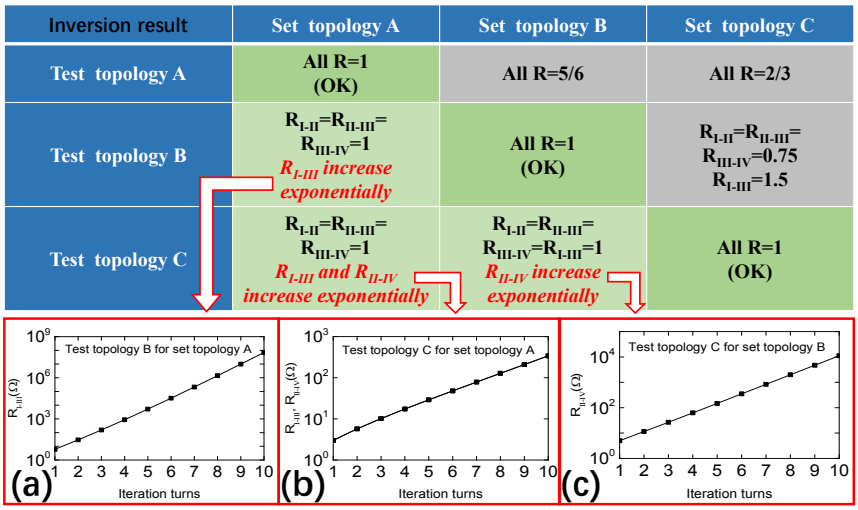

Fig. 4. Martrix show of inverse result for mixed topologies. When test topology matches the set topology by coincidence, shown in the diagonal cell of the table, inversion process can be performed normally, but error could happen as the test topology is oversimplified. If test topology is more complicated than set topology, excess inversed components go divergent, as show in (a) divergence of excess resistance between node I and III of test topology B for set topology A, (b) divergence of excess resistance between node I(II) and III(IV) of test topology C for set topology A, and (c) divergence of excess resistance between node II and IV of test topology C for set topology B

4.3 Inversion with Admittance

The potential application of RECAP is actually not only in pure loss networks, so the current section discusses electromagnetic inversion with energy storage elements. In order to focus on the inversion of reactive components, the number of nodes used for the inversion of reactive components is set to three, and only typical circuit units are discussed, that is, capacitors with resistors in parallel and inductors with resistors in series as inversion units. As shown in Fig. 6, the circuit to be inversed and the RECAP inversion circuit are shown in Fig. 6a and Fig. 6b, respectively. The RECAP tool is composed of three nodes. The variable unit between each two nodes is composed of four components, saying variable capacitors with variable resistance in parallel, and variable inductance with resistance in series. The RECAP inversion process and results are presented in the table in the lower left corner of Fig. 6. In order to highlight the inversion of the reactive element, the inversion process of the resistance element is not displayed. It can be noticed that there are a total of 12 components in three nodes to be inverted. It seems that the amount of information available for inversion is too small. However, there is no problem in principle by making full use of frequency dependent complex impedance measurement in the inversion process of reactance components. In order to focus on the feasibility of the RECAP inversion of reactance, this article does not involve the problem of mining as many circuit components in unit as possible from the complex impedance spectrum, but only the lower frequency of 100 Hz and the higher frequency of 1

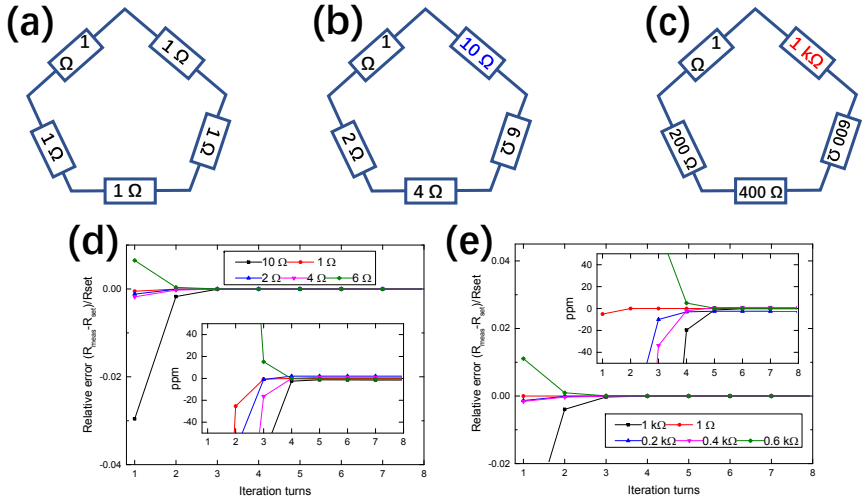

Fig. 5. Convergence process dependence of resistance differences for the same topology, where maximum to minimum ratio is equal to (a) 1 (b) 10 and (c) 1000. The convergence of the (a) is obviously one-step convergence, while the convergence process of (b) and (c) is shown in (d) and (e), respectively.

MHz is chosen for inversion tests. The complex impedance of the dual frequency point is implemented here by LCR measurement. At each frequency point one can inverse two component parameters by complex impedance measurement, so dual frequency measurement results of the three nodes can achieve exactly 12 component parameters in total. It is not difficult to understand that the inductance element has obvious contribution to impedance at high frequencies but less contribution to impedance at low frequencies, which is equivalent to being short-circuited. Capacitive elements have a greater contribution to impedance at low frequencies, but are similar to being short-circuited at high frequencies. Therefore, this work uses in-parallel RC measurement at 100 Hz for the separate inversion of parallel resistance and parallel capacitance, and the series RL measurement result at 1 MHz corresponds to the separate inversion of series inductance and series resistance. Like the simulation example discussed in the second section of this paper, the first row of data in the inversion process table in Fig. 6 is the set component parameters, the second row of data is the capacitance or inductance corresponding to the two-node measurement results, and the third row is initialization result. Nodes pair with the largest impedance modulus among the three-node combination was chosen for initialization of the high and low frequency components. That means, initialization starts from the parallel capacitors at the III-I node with the smallest capacitance at 100 Hz (the parallel resistance is not introduced when the parallel capacitor is initialized, and all the The series inductance and series resistance are short-circuited), and then the parallel resistance is initialized similarly to the method. The series inductance is initialized at the II-III node with the largest inductance at 1 MHz. Then similar rules were used to initialize the series resistance. After initialization, the parallel capacitance measured at 100 Hz and the series inductance measured at 1 MHz between each two nodes are 667 nF and 2.57 mH, respectively. After initialization, the first iteration of RECAP also follows the parallel capacitance of the I-II node at 100 Hz, the parallel resistance at 100 Hz, the series inductance and the series resistance at 1 MHz; then the II-III node and the III-I node. After each round of inversion, whether the next round of RECAP inversion iteration is also determined by whether the average relative error is less than the set limit. This paper found that the inversion of a three-node parallel RC plus series RL element can be lower than the average relative error limit of 1

When checking the frequency spectra of complex impedance between node III and node I, one may find the stable convergence picture as shown in Fig. 7. Because the initialization process begins from the low-frequency capacitance between node III and I, initial parameters of the components between other nodes deviate greatly from the set value. Therefore, initially only the complex impedance spectrum at the low-frequency point is consistent with that of the set parameters, while it completely deviates from the multiple turning characters in the middle frequency range due to LC resonances. As the RECAP iterative process progresses, from the first round, the second round to the fourth round, the turning curves in the middle steadily approaches the complex impedance spectrum of set parameters. After the fourth round of inversion iteration, there is

no obvious difference between the RECAP result and the frequency spectrum of set parameters from the spectrum comparison. When we check the convergence process of multiple iterations, as shown in Fig. 8, the two curves of solid circles and open squares respectively represent the average relative error between the component parameter and the set parameter and the LCR testing result of corresponding node pairs. The relative error of the component parameters is obviously greater than the relative error of the AC properties of the corresponding node pair, because the adjustment of the component parameter is based on the measurement and comparison results of the AC performance between the every node pair, and the primary measurement comparison error is amplified. However, from the average relative error attenuation curve of the component parameters. It can also be seen that at the fourth round of RECAP, the coarse component self-adjustment is transformed into the fine adjustment of components, thereby gradually approaching the set value. It is not difficult to see that after the 12th cycles of iteration, the average relative error afterwards is close to one thousandth.

4.4 Complexity Analysis

Inversion efficiency and process complexity are very important indicators for application. From the instances demonstrated in previous sections, it is found that

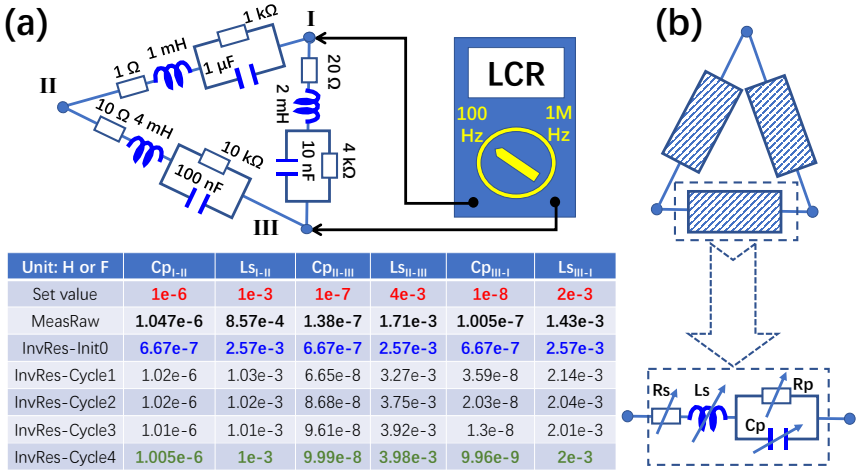

Unit: H or F	Cp_{I-II}	Ls_{I-II}	Cp_{II-III}	Ls_{II-III}	Cp_{III-I}	Ls_{III-I}
Set value	1e-6	1e-3	1e-7	4e-3	1e-8	2e-3
MeasRaw	1.047e-6	8.57e-4	1.38e-7	1.71e-3	1.005e-7	1.43e-3
InvRes-Init0	6.67e-7	2.57e-3	6.67e-7	2.57e-3	6.67e-7	2.57e-3
InvRes-Cycle1	1.02e-6	1.03e-3	6.65e-8	3.27e-3	3.59e-8	2.14e-3
InvRes-Cycle2	1.02e-6	1.02e-3	8.68e-8	3.75e-3	2.03e-8	2.04e-3
InvRes-Cycle3	1.01e-6	1.01e-3	9.61e-8	3.92e-3	1.3e-8	2.01e-3
InvRes-Cycle4	1.005e-6	1e-3	9.99e-8	3.98e-3	9.96e-9	2e-3

Fig. 6. A typical circuit including inductors and capacitors for inverse demonstration, where capacitance with resistance in parallel and inductance with resistance in series is measured at 100 Hz and 1 MHz, respectively, for node pair from I to II, from II to III and from III to I. Then the entire measurement result is input to the reconfigurable circuit network. Under the RECAP inverse strategy, after 4 runs of auto adjustment, the inverse circuit inverses the set parameters within 1 percent uncertainty.

the RECAP method directly compares the measurement results of the learning circuits with the inversed circuit, and the entire process is truly observable. Moreover, it is easy to be understood in real physical scenes. That is not like normal numerical methods which convert the measured results in the real physical world into a digital mode, and at the end of the inversion, it is converted back into observable and understandable data for the real physical world. The intermediate processed data is difficult to be directly accessable by the real world. In addition, from previous examples, it can be seen that RECAP's dependence on the time or space resources required for inversion increases linearly with the increase of number of elements N, because the number of iterations is limited (about 3-5 rounds based on examples in this article), a total of N operations are performed on the variable elements one by one in each round. Furthermore, if block or hierarchical designs are introduced in future, there is still potential for improvement, which is more attractive than the usual inversion algorithm with the super-linear dependence of N. Therefore, from the perspective of better comprehensibility and resource consumption dependency, RECAP does provide a new, simpler and more direct way for inversion.

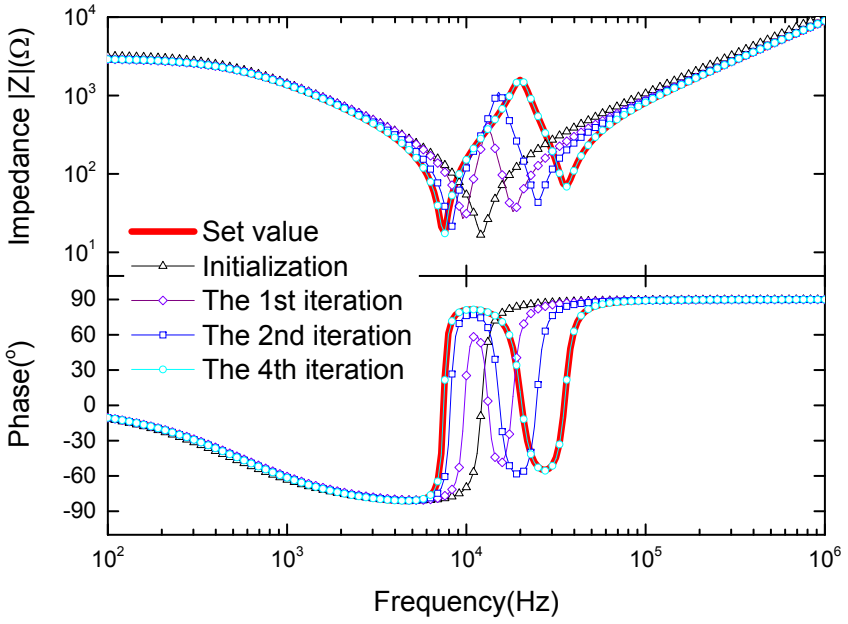

Fig. 7. Frequency spectrum of impedance modulus and phase between the node I and III during the different cycles, with comparison to corresponding spectrum of set components and initialized components before RECAP.

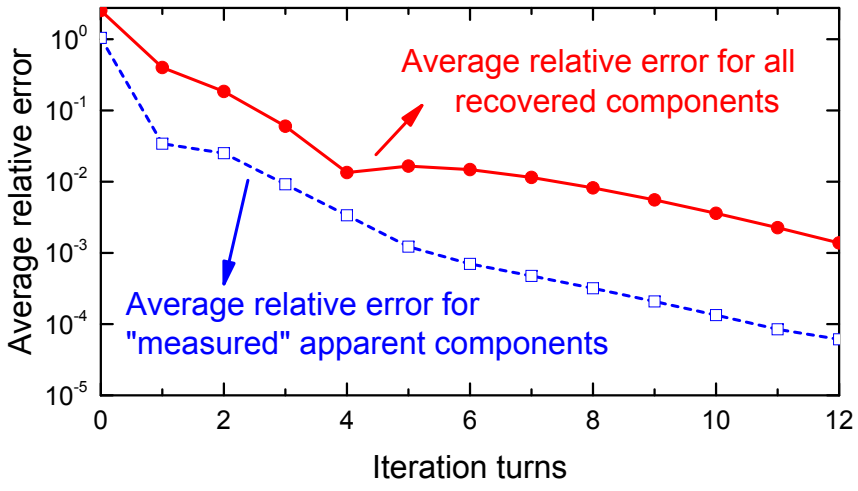

Fig. 8. Convergence behavior of average relative error for recovered components and measured apparent components during the RECAP inversion process.

5 Conclusion

This paper proposes a reconfigurable circuit auto-processing method for electromagnetic inversion. The method uses the measured properties of the inversed circuit as a criterion, automatically adjusts the component parameters, and gradually approximates the inversed circuit component parameters after several iterations. Through several simulation demonstrations of typical circuit inversion, this method shows high accuracy and stable convergence ability, and can help judge and optimize whether the topology is suitable. This method can not only inverse purely loss components, but also inverse circuits containing reactive components. Based on the verification from cases, it is also found that the inversion efficiency of RECAP is linearly dependent on the number of elements N, which is better than the usual mature inversion algorithms. RECAP combines precision measurement and circuit flexibility with switchable topology, avoiding the complicated transformation between the real world and mathematical forms of pure numerical or digital methods, and provides a new type of efficient and fast hardware for solving simulation and inversion for real world problems. This method is expected to be used to guide the design and verification of direct inversion with integrated processing chips.

References

1. Bao, G., Ammari, H., Fleming, J.: An inverse source problem for maxwell's equations in magnetoencephalography. SIAM Journal on Applied Mathematics **62**(4), 1369–1382 (2002), https://doi.org/10.1137/S0036139900373927

2. Benner, P., Mach, T.: The preconditioned inverse iteration for hierarchical matrices. Numerical Linear Algebra with Applications **20**(1), 150–166 (2013). https://doi.org/10.1002/nla.1830, http://doi.wiley.com/10.1002/nla.1830
3. Bikowski, J., Knudsen, K., Mueller, J.: Direct numerical reconstruction of conductivities in three dimensions using scattering transforms. Inverse Problems **27**(1), 015002 (2011). https://doi.org/10.1088/0266-5611/27/1/015002, https://iopscience.iop.org/article/10.1088/0266-5611/27/1/015002
4. Calderon, A.P.: On an inverse boundary value problem. ATAS of SBM (Rio de Janeiro) **1980**, 65 (1980), https://www.scielo.br/pdf/cam/v25n2-3/a02v2523.pdf
5. Chapman, J., Batson, P., Waddell, E., Ferrier, R.: The direct determination of magnetic domain wall profiles by differential phase contrast electron microscopy. Ultramicroscopy **3**, 203 – 214 (1978). https://doi.org/https://doi.org/10.1016/S0304-3991(78)80027-8, http://www.sciencedirect.com/science/article/pii/S0304399178800278
6. Christen, J., Fox, C.: Markov chain monte carlo using an approximation. Journal of Computational and Graphical Statistics **14**(4), 795–810 (2005). https://doi.org/10.1198/106186005X76983, http://www.tandfonline.com/doi/abs/10.1198/106186005X76983
7. Close, R., Chen, Z., Shibata, N., Findlay, S.: Towards quantitative, atomic-resolution reconstruction of the electrostatic potential via differential phase contrast using electrons. Ultramicroscopy **159**, 124 – 137 (2015). https://doi.org/https://doi.org/10.1016/j.ultramic.2015.09.002, http://www.sciencedirect.com/science/article/pii/S0304399115300255
8. Cultrera, A., Callegaro, L.: Electrical resistance tomography of conductive thin films. IEEE Transactions on Instrumentation and Measurement **65**(9), 2101–2107 (2016). https://doi.org/10.1109/TIM.2016.2570127, http://ieeexplore.ieee.org/document/7484320/
9. Dickin, F., Wang, M.: Electrical resistance tomography for process applications. Measurement Science and Technology **7**(3), 247–260 (1996), https://doi.org/10.1088%2F0957-0233%2F7%2F3%2F005
10. Engl, H., M., H., Neubauer, A.: Regularization of Inverse Problem. Kluwer Academic Publishers, Boston (1996)
11. Gehre, M., Jin, B., Lu, X.: An analysis of finite element approximation in electrical impedance tomography. Inverse Problems **30**(4), 045013 (2014). https://doi.org/10.1088/0266-5611/30/4/045013, https://iopscience.iop.org/article/10.1088/0266-5611/30/4/045013
12. Hähnlein, C., Schilcher, K., Sebu, C., Spiesberger, H.: Conductivity imaging with interior potential measurements. Inverse Problems in Science and Engineering **19**(5), 729–750 (2011). https://doi.org/10.1080/17415977.2011.598522, http://www.tandfonline.com/doi/abs/10.1080/17415977.2011.598522
13. Jifu, H., Ke, W.: A unified tlm model for wave propagation of electrical and optical structures considering permittivity and permeability tensors. IEEE Transactions on Microwave Theory and Techniques **43**(10), 2472–2477 (1995). https://doi.org/10.1109/22.466182, http://ieeexplore.ieee.org/document/466182/
14. Lambot, S., Slob, E., van, d., Stockbroeckx, B., Vanclooster, M.: Modeling of ground-penetrating radar for accurate characterization of subsurface electric properties. IEEE Transactions on Geoscience and Remote Sensing **42**(11), 2555–2568 (2004). https://doi.org/10.1109/TGRS.2004.834800, http://ieeexplore.ieee.org/document/1356068/
15. Langer, R.: An inverse problem in differential equations. Bull. Amer. Math. Soc. **39**(10), 814 (1933), https://projecteuclid.org/euclid.bams/1183496974

16. Li, X., Zhou, Y., Wang, J., Wang, Q., Lu, Y., Duan, X., Sun, Y., Zhang, J., Liu, Z.: A novel deep neural network method for electrical impedance tomography. Transactions of the Institute of Measurement and Control **41**(14), 4035–4049 (2019). https://doi.org/10.1177/0142331219845037, http://journals.sagepub.com/doi/10.1177/0142331219845037
17. Liu, S., Jia, J., Zhang, Y., Yang, Y.: Image reconstruction in electrical impedance tomography based on structure-aware sparse bayesian learning. IEEE Transactions on Medical Imaging **37**(9), 2090–2102 (2018). https://doi.org/10.1109/TMI.2018.2816739, https://ieeexplore.ieee.org/document/8327855/
18. Murai, T., Kagawa, Y.: Electrical impedance computed tomography based on a finite element model. IEEE Transactions on Biomedical Engineering **Bme-32**(3), 177–184 (1985). https://doi.org/10.1109/TBME.1985.325526, http://ieeexplore.ieee.org/document/4122023/
19. Nachman, A.: Global uniqueness for a two-dimensional inverse boundary value problem. The Annals of Mathematics **143**(1), 71 (1996). https://doi.org/10.2307/2118653, https://www.jstor.org/stable/2118653?origin=crossref
20. Nielsen, M., Chuang, I.: Quantum computation and quantum inofrmation. Cambridge University Press, Cambridge (2000)
21. Norton, S., Bowler, J.: Theory of eddy current inversion. Journal of Applied Physics **73**(2), 501–512 (1993). https://doi.org/10.1063/1.353359, http://aip.scitation.org/doi/10.1063/1.353359
22. Pascual-Marqui, R., Lehmann, D., Koukkou, M., Kochi, K., Anderer, P., Saletu, B., Tanaka, H., Hirata, K., John, E., Prichep, L., Biscay-Lirio, R., Kinoshita, T.: Assessing interactions in the brain with exact low-resolution electromagnetic tomography. Philosophical Transactions of the Royal Society A: Mathematical, Physical and Engineering Sciences **369**(1952), 3768–3784 (2011). https://doi.org/10.1098/rsta.2011.0081, https://royalsocietypublishing.org/doi/10.1098/rsta.2011.0081
23. Rehman, O., Rehman, S., Tu, S., Khan, S., Waqas, M., Yang, S.: A quantum particle swarm optimization method with fitness selection methodology for electromagnetic inverse problems. IEEE Access **6**, 63155–63163 (2018). https://doi.org/10.1109/ACCESS.2018.2873670, https://ieeexplore.ieee.org/document/8481528/
24. Ren, H., Zhao, Y., Chen, S., Yang, L.: A comparative study of lumped equivalent circuit models of a lithium battery for state of charge prediction. International Journal of Energy Research (2019). https://doi.org/10.1002/er.4759, https://onlinelibrary.wiley.com/doi/abs/10.1002/er.4759
25. Selleri, S.: Genetic algorithms for the automatic synthesis of equivalent lumped-element circuits. Microwave and Optical Technology Letters **29**(5), 356–359 (2001), https://onlinelibrary.wiley.com/doi/abs/10.1002/mop.1177
26. Soleimani, M., Lionheart, W.: Absolute conductivity reconstruction in magnetic induction tomography using a nonlinear method. IEEE Transactions on Medical Imaging **25**(12), 1521–1530 (2006). https://doi.org/10.1109/TMI.2006.884196, http://ieeexplore.ieee.org/document/4016173/
27. Somersalo, E., Cheney, M., Isaacson, D., Isaacson, E.: Layer stripping: a direct numerical method for impedance imaging. Inverse Problems **7**(6), 899–926 (1991), https://doi.org/10.1088%2F0266-5611%2F7%2F6%2F011

28. Sylvester, J., Uhlmann, G.: A global uniqueness theorem for an inverse boundary value problem. The Annals of Mathematics **125**(1), 153 (1987). https://doi.org/10.2307/1971291, https://www.jstor.org/stable/1971291?origin=crossref
29. Vauhkonen, M., Kaipio, J., Somersalo, E., Karjalainen, P.: Electrical impedance tomography with basis constraints. Inverse Problems **13**(2), 523–530 (1997). https://doi.org/10.1088/0266-5611/13/2/020, https://iopscience.iop.org/article/10.1088/0266-5611/13/2/020
30. Wang, K., 2009 Fifth International Conference on Semantics, Knowledge and Grid: An encrypt and decrypt algorithm implementation on fpgas (2009). https://doi.org/10.1109/SKG.2009.74, http://ieeexplore.ieee.org/document/5370112/
31. Xu, Y., He, B.: Magnetoacoustic tomography with magnetic induction (mat-mi). Physics in Medicine and Biology **50**(21), 5175–5187 (2005). https://doi.org/10.1088/0031-9155/50/21/015, https://iopscience.iop.org/article/10.1088/0031-9155/50/21/015
32. Zhu, L., Wu, K.: Numerical de-embedding procedure and unified circuit model for planar integrated circuits. In: Hwu, R.J., Wu, K. (eds.) Terahertz and Gigahertz Photonics. vol. 3795, pp. 400 – 411. International Society for Optics and Photonics, SPIE (1999). https://doi.org/10.1117/12.370186, https://doi.org/10.1117/12.370186